Electric Fields Due to Synaptic Currents Sharpen Excitatory Transmission

Science. Author manuscript; available in PMC 2009 May 21.

Published in final edited form as:
Science. 2008 March 28; 319(5871): 1845–1849. doi:10.1126/science.1154330.

Electric Fields Due to Synaptic Currents Sharpen Excitatory Transmission

Sergiy Sylantyev[1,†], **Leonid P. Savtchenko**[1,2,†], **Yin-Ping Niu**[3,†], **Anton I. Ivanov**[4,†], **Thomas P. Jensen**[1,†], **Dimitri M. Kullmann**[1], **Min-Yi Xiao**[3], and **Dmitri A. Rusakov**[1,*]

[1]Institute of Neurology, University College London, Queen Square WC1N 3BG, London, UK.

[2]Laboratory of Biophysics and Bioelectronics, Dnepropetrovsk National University, Ukraine.

[3]Institute of Neuroscience and Physiology, Göteborg University, Sweden;

[4]INMED-INSERM U29, Marseille, France

Abstract

The synaptic response waveform, which determines signal integration properties in the brain, depends on the spatiotemporal profile of neurotransmitter in the synaptic cleft. Here, we show that electrophoretic interactions between AMPA-receptor-mediated excitatory currents and negatively charged glutamate molecules accelerate the clearance of glutamate from the synaptic cleft, speeding-up synaptic responses. This phenomenon is reversed upon depolarization and diminished when intra-cleft electric fields are weakened through a decrease in the AMPA receptor density. In contrast, the kinetics of receptor-mediated currents evoked by direct application of glutamate are voltage-independent, as are synaptic currents mediated by the electrically neutral neurotransmitter GABA. Voltage-dependent temporal tuning of excitatory synaptic responses may thus contribute to signal integration in neural circuits.

Although ion currents through postsynaptic receptors are small (~10^{-11} A), they can exert a lateral voltage gradient (electric field) of ~10^4 V/m inside the synaptic cleft (1, 2) raising the possibility that they can affect the dwell time of electrically charged neurotransmitters (3). Does electrodiffusion therefore play any role in synaptic transmission?

The excitatory neurotransmitter glutamate is negatively charged at physiological pH (pK = 4.4), implying that postsynaptic depolarization should in principle retard its escape from the synaptic cleft (Fig. 1, A). AMPA-receptor-mediated excitatory postsynaptic currents (AMPAR EPSCs) decay more slowly at positive than at negative holding voltages in hippocampal basket cells (4) and in cerebellar granule cells (5). However, this has not been reported for AMPAR EPSCs generated at perisomatic synapses on CA1 or CA3 pyramidal cells (6-8). We evoked dendritic AMPAR EPSCs in CA1 pyramidal cells by stimulating Schaffer collaterals: the EPSC decay time T (defined here as the area/peak ratio) increased monotonically with depolarization (Fig. 1, B). The ratio between T recorded at +40 mV and at −70 mV (T_{+40}/ T_{-70}) was consistently above one (average ± SEM: 2.17 ± 0.09, n = 49, $p < 0.001$; fig. S1, A). This asymmetry was independent of the EPSC amplitude, glutamate transport or recording temperature, and could not be accounted for by unknown voltage-dependent properties of receptor antagonists (fig. S1, A and B).

* To whom correspondence should be addressed. Email: d.rusakov@ion.ucl.ac.uk.
† These authors contributed equally to this work

Europe PMC Funders Author Manuscripts

A trivial possible explanation for this phenomenon is that AMPARs themselves have voltage-dependent kinetics. This has indeed been reported for AMPARs activated by brief pulses of glutamate applied to outside-out patches excised from brainstem neurons (9, 10), but not from hippocampal or dentate granule neurons (*11*). We confirmed that the decay of AMPAR currents evoked by 1 ms / 1 mM glutamate pulses in outside-out patches excised from somata (n = 9) or dendrites (n = 6) of CA1 pyramidal cells was indistinguishable at positive and negative voltages. Symmetrical decay kinetics were also observed when the AMPAR density was decreased in the patch with 0.1 μM NBQX (Fig. 1, C).

How can the slowed EPSCs at positive voltages observed here be reconciled with the reported voltage independence of the EPSC decay in CA1 pyramidal cells (6)? A possible explanation is that EPSCs in previous studies were mainly elicited at proximal synaptic inputs, to ensure optimal voltage clamp (6, 12, 13). Because in CA1 pyramidal cells the density of dendritic synaptic AMPARs increases with the distance from the soma (12-14), the influence of intra-cleft electric fields on glutamate may be far smaller at perisomatic synapses. To determine whether this explanation is plausible, we simulated the motion of glutamate molecules in the characteristic environment of small hippocampal synapses. Our Monte Carlo approach (15) was broadly consistent with previous models (16, 17), with the difference that, at each elemental time step dt, each molecule underwent a small displacement due to the local electric field generated by the currents flowing through postsynaptic AMPARs (18). Classically, this displacement is given by $-Dq\frac{F}{RT}\mathbf{E}dt$, where $\mathbf{E}$ is the electric field (15), D is the diffusion coefficient (19), $q = -1$ for glutamate, F is Faraday's constant, R is the gas constant, and T is temperature. The simulations confirmed that reversal of the AMPAR-mediated synaptic current (by switching to a positive membrane potential) retards the rate of escape of glutamate from the cleft, and consequently slows the EPSC decay (Fig. 1, D; fig. S2, A and B). This effect is consistent with the experimentally observed voltage asymmetry of T and depends strongly on the number of available synaptic AMPARs (Fig. 1, E; fig. S2, C). When N is relatively high (>20 open AMPARs at the peak), the effect of electrodiffusion is comparable with that of a two-fold change in the glutamate diffusion coefficient (fig. S3). Conversely, the predicted voltage asymmetry of T is much smaller when N is lower, as expected for proximal synapses.

To test experimentally if reducing the density of activated AMPARs indeed attenuates the voltage asymmetry of T, we evoked EPSCs at different dendritic locations while visualizing the stimulating pipette position with two-photon excitation microscopy (Fig. 2, A). We confirmed that stimulation stochastically evoked synaptic events in dendritic spines (fig. S4). Having documented the T_{+40}/T_{-70} ratio in baseline conditions, we blocked a proportion of AMPARs by 0.1 μM NBQX which decreased the EPSC amplitude by 40 ± 4% (n = 7; Fig. 2, B). Because this decrease could also alter voltage clamp conditions of our recordings, we increased the stimulus strength to restore the EPSC amplitude to its baseline value (we thus recruited more local synapses operating at lower AMPAR densities; Fig. 2, B). At all dendritic sites >100 μm from the soma, partial AMPAR blockade substantially reduced the T_{+40}/T_{-70} ratio (by 37 ± 5%, n = 7, $p < 0.005$; Fig. 2, C). In contrast, at more proximal sites, this ratio was initially much smaller than that at distal sites (1.30 ± 0.06 and 2.30 ± 0.18, n = 4 and n = 7, respectively; $p < 0.003$) and it was not altered by NBQX application even though the EPSC amplitude was reduced to the same degree as at distal sites (by 39 ± 3%, n = 4; Fig. 2, D). Because a reduction in AMPAR density has no effect on receptor kinetics in outside-out patches (Fig. 1, C), our observations are consistent with intra-cleft electric fields decelerating glutamate escape from the cleft upon depolarization at distal, but not proximal excitatory synapses in CA1 pyramidal cells.

We designed an alternative approach to test whether the average dwell time of intra-cleft glutamate following exocytosis is greater at positive than at negative holding voltages (Fig. 1, D). If this is indeed case, the rapidly dissociating competitive antagonist γ-D-glutamylglycine (γ-DGG) should block a higher fraction AMPARs at negative than at positive voltages (16, 20, 21), as predicted by modeling (Fig. 3, A). First, we confirmed that the kinetics of AMPAR-mediated currents evoked by a brief glutamate pulses in outside-out patches in 0.5 mM γ-DGG were voltage-independent (Fig. 3, B). In keeping with our prediction, the reduction of AMPAR EPSC amplitudes by 0.5 mM γ-DGG was 20 ± 7 % greater at negative than at positive holding voltages ($n = 8$, $p < 0.02$; Fig. 3, C and D). Blocking glutamate uptake with 50 μM TBOA, to rule out any possible contribution of voltage-dependent transporters, increased this difference to 45 ± 16 % ($n = 18$, $p < 0.001$; Fig. 3, D) while reducing the overall effects of 0.5 mM γ-DGG, probably due to an increase in the ambient level of glutamate. In contrast, 0.1 μM NBQX reduced the EPSC amplitude equally at both positive and negative holding voltages, in accordance with modeling predictions (fig. S5). These results further confirm that the sign of the synaptic current influences the rate of escape of glutamate from the synaptic cleft.

Finally, if synaptic currents do influence glutamate diffusion, holding the postsynaptic cell at the receptor reversal potential (zero current) and immediately after presynaptic glutamate release should abolish the effect of voltage on EPSC decay. We therefore switched the holding voltage from the AMPAR reversal potential (0 mV) to either −70 mV or +40 mV during the EPSC decay phase (Fig. 3, E) and compared the outcome with the EPSCs recorded without the voltage jump. The voltage-jump responses showed a 20 ± 5% slower decay at −70 mV ($p < 0.005$, $n = 11$), and a 34 ± 10% faster decay at +40 mV ($p < 0.01$, $n = 12$; Fig. 3, F) (18). The EPSC waveform was thus influenced by the recent history of current flow (22), consistent with electrodiffusion.

Does electrodiffusion of glutamate influence the activation of other receptors? High-affinity NMDA receptors (NMDARs) both within and outside synapses may be activated by synaptic releases of glutamate (23, 24). This, in addition to voltage-dependent blockade by Mg^{2+}, is likely to mask the effects of electrodiffusion on NMDAR responses. Nevertheless, we observed a voltage-dependent asymmetry of NMDAR EPSCs in the absence of extracellular Mg^{2+} in cultured hippocampal neurons, which are not surrounded by dense neuropil (Fig. 4, A; figs. S6 and S7). This was again consistent with modeling (fig. S8). In contrast, a relatively low concentration of glutamate applied diffusely to the dendrites - to activate NMDARs at a lower density - evoked responses that showed voltage-independent kinetics but otherwise were similar to those evoked synaptically (Fig. 4, A; fig. S9). Furthermore, reduction of NMDAR EPSCs by the fast-dissociating competitive antagonist Daminoadipate (D-AA) was greater at negative than at positive voltages (fig. S10). Finally, both slowly- and fast-dissociating NMDAR antagonists, 0.4 μM D-CPP and 50 μM D-AA, reduced the voltage-dependent asymmetry of τ (fig. S11).

These phenomena should play no role in the activation of $GABA_A$ receptors because GABA is a zwitterion. We tested this prediction in neuronal cultures, again, to avoid the confounding effects of extrasynaptic and/or tonically active $GABA_A$ receptors in slices. Although $GABA_A$ receptor-mediated IPSCs did decelerate at positive voltages (with respect to the Cl^- reversal potential), the responses were symmetrical when GABA transporters were blocked with 25 μM SKF-89976A (Fig. 4, B). Thus, we observed no evidence that electric fields affect the synaptic dwell time of GABA.

Electrodiffusion of glutamate thus may explain, at least in part, why AMPAR EPSCs at some central synapses are retarded by depolarization (4, 5) and why EPSCs recorded locally at distal dendrites of CA1 pyramidal cells have faster decays than those at proximal

dendrites (12). The extent of this phenomenon is likely to vary among synapses, depending for instance on the density or numbers of synaptic receptors. Although electrodiffusion is thus a fundamental feature of AMPAR-mediated synaptic transmission, does it play a physiologically significant role in synaptic signal integration? Distal dendrites of pyramidal neurons can undergo extensive depolarization (including spiking) without exciting the soma (25) (Fig. 4, C), and even modest changes in τ due to electrodiffusion should in principle affect the time interval over which the input coincidence triggers an action potential. Indeed, simulations with a NEURON (26) model of a CA1 pyramidal cell (12, 27) suggest that, for an arbitrary sample of Schaffer collateral input locations (Fig. 4, C), a ~20% shortening of the synaptic conductance decay could reduce the coincidence detection window by 52 ± 6 % ($n = 16$, $p < 0.001$; Fig. 4, D). Another potential consequence of electrodiffusion is that local postsynaptic depolarization, by extending the dwell time of intra-cleft glutamate (Fig. 1, D), may enhance activation of NMDARs. This is likely to interact synergistically with the depolarization-dependent attenuation of postsynaptic glutamate transport (16) and relief of Mg^{2+} block, thus potentially facilitating induction of NMDAR-dependent synaptic plasticity.

Supplementary Material

Refer to Web version on PubMed Central for supplementary material.

Acknowledgments

We thank Bengt Gustafsson and Eric Hanse for their comments and support. This work was supported by the Wellcome Trust, the MRC (UK), EU (Promemoria 512012) and HFSP (RGP50/2006), and also by the Swedish Research Council, the Swedish Society of Medicine and the Göteborg Medical Society.

References and Notes

1. Eccles JC, Jaeger JC. Proc. R. Soc. Lond. B. 1958; 148:38. [PubMed: 13494474]
2. Savtchenko LP, Antropov SN, Korogod SM. Biophys J. 2000; 78:1119. [PubMed: 10692302]
3. Takeuchi A, Takeuchi N. J Neurophysiol. 1959; 22:395. [PubMed: 13673292]
4. Kneisler TB, Dingledine R. Hippocampus. 1995; 5:151. [PubMed: 7550611]
5. Cathala L, Holderith NB, Nusser Z, DiGregorio DA, Cull-Candy SG. Nature Neurosci. 2005; 8:1310. [PubMed: 16172604]
6. Hestrin S, Nicoll RA, Perkel DJ, Sah P. J Physiol. 1990; 422:203. [PubMed: 1972190]
7. McBain C, Dingledine R. J Neurophysiol. 1992; 68:16. [PubMed: 1355525]
8. Jonas P, Major G, Sakmann B. J. Physiol. 1993; 472:615. [PubMed: 7908327]
9. Raman IM, Trussell LO. Biophys J. 1995; 69:1868. [PubMed: 8580330]
10. Veruki ML, Morkve SH, Hartveit E. J Physiol. 2003; 549:759. [PubMed: 12702738]
11. Colquhoun D, Jonas P, Sakmann B. J Physiol. 1992; 458:261. [PubMed: 1338788]
12. Magee JC, Cook EP. Nat Neurosci. 2000; 3:895. [PubMed: 10966620]
13. Andrasfalvy BK, Magee JC. J Neurosci. 2001; 21:9151. [PubMed: 11717348]
14. Nicholson DA, et al. Neuron. 2006; 50:431. [PubMed: 16675397]
15. Savtchenko LP, Rusakov DA. Proc Natl Acad Sci U S A. 2007; 104:1823. [PubMed: 17261811]
16. Diamond JS. J Neurosci. 2001; 21:8328. [PubMed: 11606620]
17. Franks KM, Bartol TM Jr. Sejnowski TJ. Biophys J. 2002; 83:2333. [PubMed: 12414671]
18. Supporting Online Material.
19. Nielsen TA, DiGregorio DA, Silver RA. Neuron. 2004; 42:757. [PubMed: 15182716]
20. Clements JD, Lester RAJ, Tong G, Jahr CE, Westbrook GL. Science. 1992; 258:1498. [PubMed: 1359647]
21. Christie JM, Jahr CE. J Neurosci. 2006; 26:210. [PubMed: 16399689]

22. Magleby KL, Stevens CF. J Physiol. 1972; 223:151. [PubMed: 4537943]
23. Arnth-Jensen N, Jabaudon D, Scanziani M. Nature Neurosci. 2002; 5:325. [PubMed: 11896395]
24. Scimemi A, Fine A, Kullmann DM, Rusakov DA. J. Neurosci. 2004; 24:4767. [PubMed: 15152037]
25. Hausser M, Spruston N, Stuart GJ. Science. 2000; 290:739. [PubMed: 11052929]
26. Hines ML, Carnevale NT. Neuroscientist. 2001; 7:123. [PubMed: 11496923]
27. Migliore M. J Comput Neurosci. 2003; 14:185. [PubMed: 12567016]
28. Wadiche JI, Jahr CE. Neuron. 2001; 32:301. [PubMed: 11683999]

Europe PMC Funders Author Manuscripts

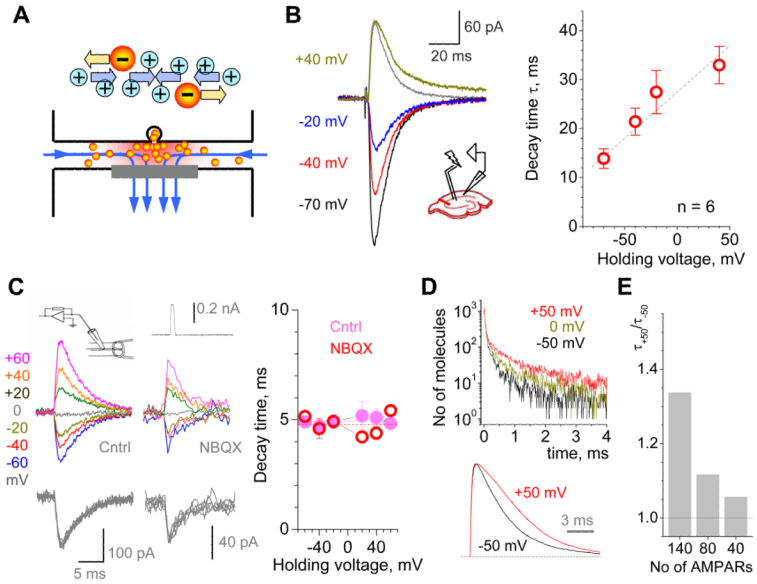

Fig. 1. Interactions between AMPAR currents and glutamate inside the synaptic cleft affect the kinetics of synaptic responses

(**A**) Schematic: negatively charged glutamate molecules experience an electrical force opposite to the cation flux. (**B**) The EPSC decay constant τ (area / amplitude) increases monotonically with depolarization. Left, example in one cell: AMPAR EPSCs recorded at four holding voltages (shown color-coded; gray line, response at −70 mV reversed and normalized to that at +40 mV). Plot, average voltage-decay relationship in six cells: mean ± SEM; dotted line, linear regression. (**C**) Left: AMPAR currents evoked in an outside-out patch by a 1 ms pulse of 1 mM glutamate (upper insets: schematic adapted from (11) and the time course of solution exchange); traces, AMPAR receptor response in baseline conditions (Cntrl, dendritic patch example) and in 0.1 μM NBQX (NBQX, somatic patch example); gray traces, same currents normalized to the amplitude at −60 mV. Graph, average τ ± SEM (Cntrl, closed circles: AMPAR kinetics from n = 9 somatic and n = 6 dendritic patches were indistinguishable and therefore pooled; NBQX, open circles: n = 7); dotted lines, global average. (**D**) Monte Carlo simulations predict that postsynaptic depolarization retards escape of glutamate from the cleft (upper panel) and prolongs AMPAR currents (lower panel; total 140 AMPARs). (**E**) In simulated AMPAR responses, the ratio τ_{+50}/τ_{-50} (ordinate) depends strongly on the number of synaptic AMPARs (abscissa).

Europe PMC Funders Author Manuscripts

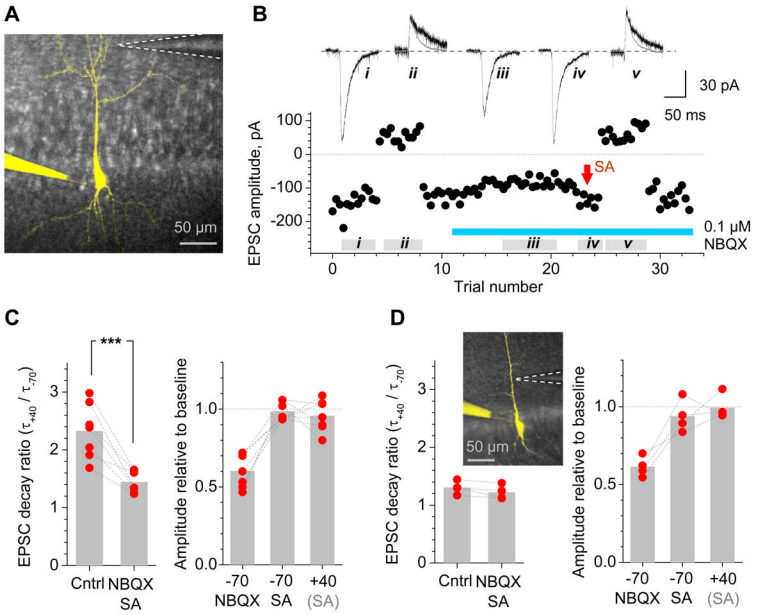

Fig. 2. The voltage-dependent asymmetry of the EPSC decay is prominent at distal, but not proximal, synapses in CA1 pyramidal cells and depends on the AMPAR density

(**A**) Stimulating pipette position (dotted lines) relative to the apical dendrites of a CA1 pyramidal cell (filled with Alexa Fluor 594, λ_x = 800 nm). (**B**) EPSCs evoked at a remote dendritic site in one cell, as shown in (A), and recorded at −70 mV and +40 mV, before and after application of 0.1 µM NBQX (blue segment); dots, EPSC amplitude; gray segments correspond to the average traces, as indicated by Roman numerals; red arrow, stimulus amplitude adjustment (SA). See text for details. (**C**) Summary of experiments shown in (B): the EPSC decay ratio T_{+40}/T_{-70} is reduced by 0.1 µM NBQX from 2.30 ± 0.18 to 1.44 ± 0.07 (left panel; n = 7, $p < 0.005$) whereas the EPSC amplitude is 0.99 ± 0.02 and 0.96 ± 0.04 of its baseline values at −70 mV and +40 mV, respectively (right panel; bars show amplitude change relative to baseline at the indicated holding voltage). (**D**) In proximal (perisomatic) synapses (inset), application of NBQX has no effect on the T_{+40}/T_{-70} ratio (baseline: 1.30 ± 0.06; NBQX: 1.22 ± 0.06, n = 4; N.S.); notations as in (C).

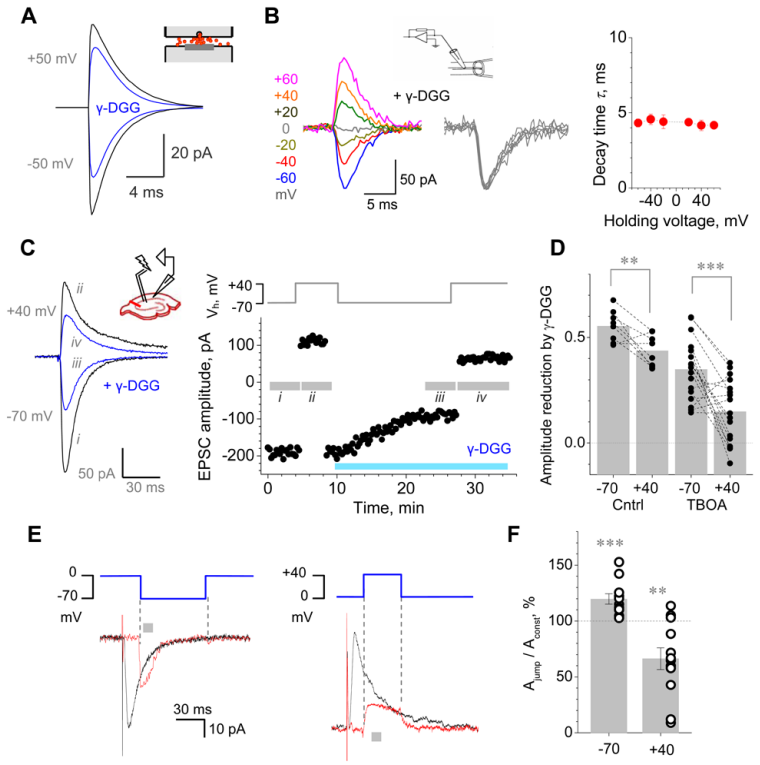

Fig. 3. Postsynaptic membrane voltage affects glutamate escape from the cleft

(**A**) Monte Carlo simulations of AMPAR EPSCs (kinetics in accordance with ref. (28), 2000 glutamate molecules released) predict that 0.5 mM γ-DGG should be less effective at positive than at negative holding voltages. (**B**) Outside-out patch experiments showing that interactions between AMPARs and γ-DGG are voltage-independent; notation as in Fig. 1, C. (**C**) In slices, reduction of AMPAR EPSCs by 0.5 mM γ-DGG is smaller at +40 mV than at −70 mV; traces, example from one cell (Roman numerals correspond to gray segments in the plot); plot, the corresponding amplitude time course; upper panel, holding voltage; blue segment, application of 0.5 mM γ-DGG; gray segments, trace averaging. (**D**) Summary of experiments shown in (C); bars, average values; connected dots, data points from individual cells. Average amplitude reduction by γ-DGG: 51 ± 3 % at −70 mV and 43 ± 3 % at +40 mV (n = 8, $p < 0.01$); in the presence of 50 μM TBOA: 35 ± 3 % and 16 ± 4 %, respectively (n = 18, $p < 0.005$). (**E**) Switching the holding voltage rapidly from the AMPAR reversal potential (~0 mV) unmasks the voltage dependence of response kinetics; one-cell examples. Black, EPSC at −70 mV (left) or +40 mV (right); red trace, synaptic response during the holding-voltage jump (blue) minus the response to the voltage jump alone (no stimulus). (**F**) Summary of experiments shown in (E): ratio between the average current amplitude over a 10 ms interval 5-10 ms after the jump onset (A_{jump}; gray segments in (E)) and the current value over the same time window when the cell is held at either −70 mV or + 40 mV throughout the sweep (A_{const}; voltage is indicated).

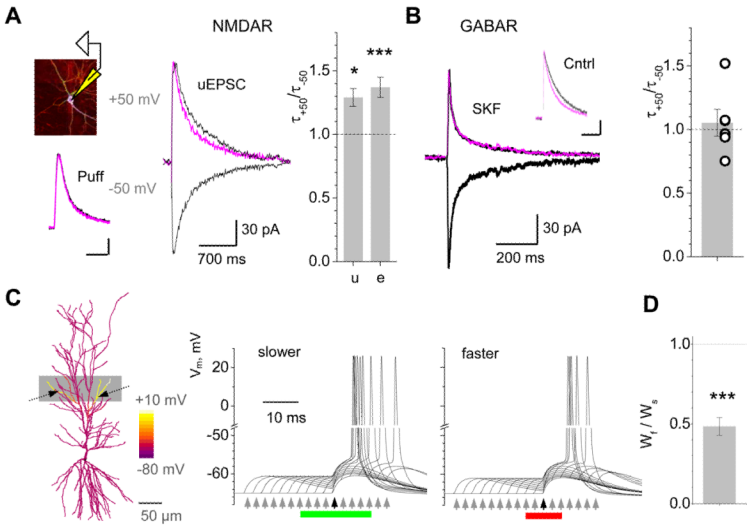

Fig. 4. Effects of electrodiffusion depend on the neurotransmitter charge and may affect signal integration properties in hippocampal neurons

(**A**) NMDAR-mediated EPSCs recorded in culture at zero Mg^{2+} (unitary EPSC, uEPSC); traces from one cell; magenta, response at −50 mV normalized to that at +50 mV. Puff, responses to a pressure pulse of glutamate (scale values apply throughout). Graph, average T_{+50}/T_{-50} ratios (± SEM) for unitary (u) and evoked (e) NMDAR EPSCs: 1.29 ± 0.07 and 1.37 ± 0.08 (n = 6, $p < 0.02$ and n = 15, $p < 0.001$, respectively; see figs. S6-S11 for further experiments). (**B**) Synaptically evoked $GABA_A$ receptor-mediated responses in culture show no voltage-dependent asymmetry in the presence of the GABA uptake blocker SKF-89976A (25 µM); Cntrl, responses before GABA uptake blockade; inward and outward current correspond to, respectively, 30 mV below and above the Cl^- reversal potential corrected for junction potential (18); other notation as in (A). Graph, summary: average T_{+50}/T_{-50} : 1.05 ± 0.10 (n = 6). (**C**) Diagram, a detailed NEURON model of a CA1 pyramidal cell (12, 27); arrows, an example of two synapses that could strongly depolarize local dendrites (and even produce local spikes) without exciting the soma (V_m color-coded); gray shadow, dendritic area of tested synaptic pairs. (**D**) Simulations illustrating coincidence detection for two synaptic inputs: one activated at time zero (black arrow) and the other activated at 3 ms intervals before and after (gray arrows). During the coincidence detection time window (red and green segments), summation generates a spike. In left and right graphs, the synaptic conductance decay set at 10 ms (slower) and 8 ms (faster), respectively, to reflect the effect of electrodiffusion. (**E**) Summary of experiments shown in (C) for arbitrarily selected synaptic input pairs: the coincidence detection window for faster versus slower inputs (W_f / W_s); mean ± SEM: 0.48 ± 0.06 ($p < 0.001$, n = 18).